Article Type: Research

OPEN ACCESS

Assessment of Soil Liquefaction Potential in Eastern Miandoab by Field Data and Empirical Relationships

Armin Mozafarbagi[1], Ebrahim Asghari-Kaljahi[1,*]

[1]Department of Earth Sciences, Tabriz University, Tabriz 5166616471, Iran
*Corresponding author: e-asghari@tabrizu.ac.ir

Received: 10 July 2024 / Accepted: 28 July 2024 / Published: 25 August 2024

***Abstract*:** Soil liquefaction is a significant geotechnical hazard that poses risks to structures during earthquakes. It occurs when loose, saturated granular soils lose shear strength under seismic forces, causing the soil to behave like a liquid and leading to structural damage. A common approach for evaluating liquefaction potential involves field testing, especially the Standard Penetration Test (SPT), combined with empirical methods. This study assesses the liquefaction potential in the eastern region of Miandoab, using data from 16 boreholes. Grain size analysis and SPT results were analyzed, and the empirical method by Iwasaki et al. (1984) was applied to assess the region's liquefaction hazard. The findings show that in the central areas, the liquefaction risk is moderate, with a hazard level close to 5. In contrast, the northern and southern sections, characterized by denser soils and lower groundwater levels, show a lower potential for liquefaction. However, in the event of strong earthquakes with accelerations above 0.30g, liquefaction is still possible. Earthquakes with magnitudes greater than 7 and accelerations exceeding 0.25g present a serious risk of liquefaction in the region. The study highlights the need for considering soil conditions and seismic activity when evaluating liquefaction risks in construction planning.

Keywords: Liquefaction, Geotechnical classification, Experimental relations, Miandoab, SPT.

I. INTRODUCTION

Soil liquefaction is a phenomenon in which saturated, loose granular soils lose their strength and stiffness when subjected to shear stress, behaving like a liquid. This stress can result from earthquake-induced shaking or a sudden change in soil stress conditions. Liquefaction occurs due to a reduction in the soil's strength and stiffness under undrained conditions, typically caused by momentary and cyclic forces (Demir & Özener, 2022). In simple terms, if the pore water pressure between soil particles becomes high enough to support the load, the soil particles may separate, causing the soil to act like quicksand. This leads to a chain reaction, where one particle's movement triggers another, eventually causing the soil to flow like a liquid. Prior to an earthquake, while the soil may be saturated, its pore water pressure is low. However, when stress is applied, the low permeability and drainage rate cause the pore water pressure to rise, overcoming the effective stress between the soil particles, leading to liquefaction (Farhangi et al., 2020). Under such conditions, the soil loses all shear strength, and its effective stress becomes zero (Cetin et al., 2018).

The mechanism behind liquefaction is largely driven by the buildup of pore water pressure between the particles of saturated soil (Youd, 2003). During an earthquake, the ground shakes, and the shear stress applied to the soil causes the loose particles to try to rearrange themselves into a denser state. However, because the soil is saturated, water within the pore spaces prevents the particles from moving freely (Zhang & Wang, 2012). This restriction causes the pore water pressure to increase rapidly. Once the pressure builds to the point where it equals the confining stress of the soil, the particles essentially lose contact with each other, and the soil behaves like a fluid (Youd, 2003). In essence, the soil undergoes a transition from a state where the solid particles are carrying the load, to one where the load is transferred to the pore water (Xu et al., 2021). This is a key distinction in understanding liquefaction: while dry soil may simply compact during shaking, saturated soil has the added complication of water being forced to carry the load (Huang et al., 2015). Because water cannot support shear stresses, the strength of the soil drops dramatically, and it flows similarly to a liquid (Xu et al., 2020). The soil's ability to bear loads is effectively reduced to zero, which explains the dramatic failure of foundations and other structures observed in liquefaction-prone areas (Zhang & Wang, 2012).

Field and laboratory tests have been developed to predict the likelihood of liquefaction in various soils. The Standard Penetration Test (SPT) and Cone Penetration Test (CPT) are commonly used in geotechnical engineering to measure the soil's resistance to penetration and to estimate its liquefaction potential (Boulanger and Idriss 2014). Engineers also consider factors like the grain size distribution, density, and the depth of the water table (Lenz & Baise, 2007). One of the most important indicators of potential liquefaction is the presence of loose, granular soils,

such as sands or silts, combined with a shallow groundwater level. These conditions, when paired with seismic activity, create a high risk for liquefaction (Baez et al., 2000). The consequences of liquefaction are not limited to structural damage alone. It can also trigger landslides, lateral spreading, and ground subsidence, which can devastate entire neighborhoods and cities (Zhao & Cai, 2015). Earthquake-induced liquefaction has caused severe damage worldwide, with notable examples being the Niigata, Chūetsu, and Kobe earthquakes in Japan, the L'Aquila earthquake in Italy, the Kocaeli and Izmir earthquakes in Turkey, and the Christchurch earthquake in New Zealand (Huang & Yu, 2013). In Iran, the Rudbar-Manjil earthquake is a key example (Asgari, 2017). To mitigate these risks, engineers employ various strategies, such as ground densification, soil stabilization, and drainage systems to reduce pore water pressure. Understanding the mechanism of liquefaction and improving methods for prevention remains a critical area of research in seismic-prone regions around the world (Huang & Yu, 2013).

Over the years, geotechnical experts have studied liquefiable soils extensively, developing a variety of field and laboratory methods to assess liquefaction potential. These include cyclic triaxial tests, dynamic triaxial tests, cyclic simple shear tests, the SPT, CPT, shear wave velocity (V_s), and Becker Penetration Test (BPT). While both laboratory and field methods are used to estimate engineering parameters, field tests are more widely accepted due to their ability to directly assess soil properties and field conditions (Ortiz-Hernández et al., 2022). In this study, field approaches and SPT results were employed to evaluate the liquefaction potential of soils in the eastern region of Miandoab. SPT tests were conducted, and penetration index variations for different boreholes in the study area were estimated. Using the empirical relationships proposed by Iwasaki et al. (1984), the liquefaction hazard in this region was analyzed.

II. Engineering Geology of Studied Location

Miandoab is a city in the West Azerbaijan Province of Iran, known for its strategic location at the junction of the Zarrineh Rud and Simineh Rud rivers. Its name, translating to 'between two rivers', reflects this unique geography, which has historically made the area fertile and suitable for agriculture. Situated in a region with a diverse climate, Miandoab enjoys abundant water resources, allowing it to support extensive crop cultivation, particularly of grains, fruits, and vegetables (Norouzi & Moghaddam, 2022). The city lies within the broader Western Alborz-Azerbaijan tectonic zone, giving it a complex geological structure with significant folding, faulting, and alluvial deposits, especially along the rivers (Andabili & Safaripour, 2022). Close to Lake Urmia, Miandoab experiences high groundwater levels and minimal soil consolidation in many areas, factors that are relevant in geotechnical studies and impact its building practices. Over time, Miandoab has developed into an important agricultural and trade center, with its natural resources and strategic location contributing to its economic growth (Vaziri et al., 2022).

The study area focuses on the eastern part of Miandoab city, located east of the Zarrineh Rud River (Azarafza & Mokhtari, 2013). Figure 1 shows the location of the study area. Structurally, Miandoab lies within the Western Alborz-Azerbaijan tectonic zone. This region has a complex geological history, characterized by extensive unconformities, folding, and faulting (Andabili & Safaripour, 2022). Eastern Miandoab is covered by Quaternary alluvial deposits, as shown in Figure 2. As illustrated, the study area primarily consists of Quaternary alluvium from the Zarrineh Rud and Lilan Chay rivers. These deposits, influenced by proximity to Lake Urmia, display a high groundwater level and have experienced minimal consolidation (Azarfaza & Mokhtari, 2013).

The tectonic activity in the Miandoab region has led to frequent earthquakes (Fazlnia, 2019), and according to the Iranian Code of Practice for Seismic Resistant Design of Buildings (also known as Iran national Code No. 2800) the area is classified as having a moderate seismic risk. The design peak ground acceleration for Miandoab is set at 0.25g by this standard, indicating a notable earthquake hazard. This seismic risk, combined with the area's soil characteristics, also suggests a significant potential for soil liquefaction, posing additional challenges for construction and infrastructure stability in the region.

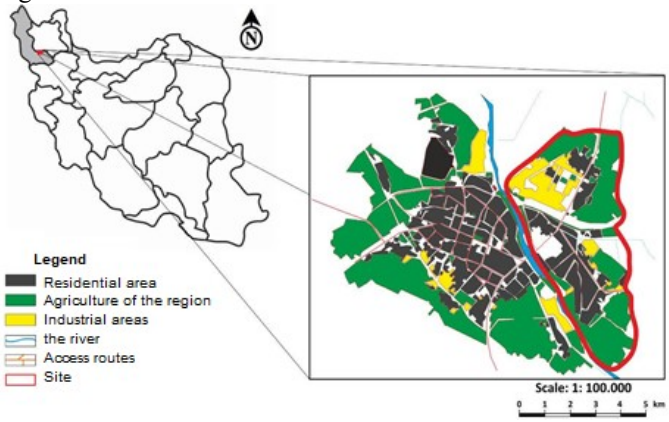

Fig. 1 Location of studied area

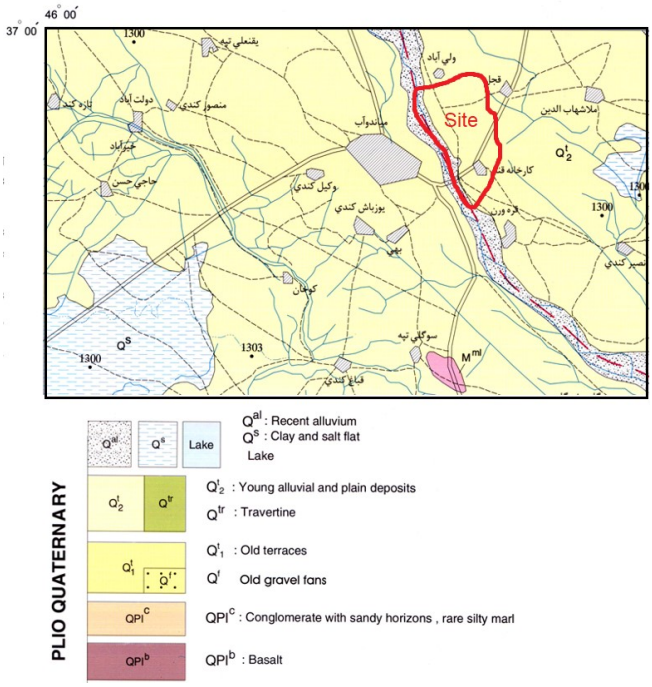

Fig. 2 Geological map for studied region
(Geological Survey and Mineral Exploration of Iran, 2009)

To assess the geotechnical conditions of eastern Miandoab, a series of local surveys and engineering geological studies were conducted, collecting data from 16 boreholes. Borehole logs indicate that the main soils in the study area consist of clay, silt, and sand. In addition to borehole sampling, soil samples were taken from several trenches in the area, followed by grain size analysis. The local soils are classified as ML (low-plasticity silt), CL (low-plasticity clay), and SM (silty sand). Figure 3 shows the grain size distribution for sandy soils in the region. Among key projects in this area is a 350-bed hospital currently in the study and construction phase, with over 10 boreholes drilled at the site. Figure 4 presents the geotechnical cross-section for this hospital site. The groundwater depth in the study area ranges from 6 to 10m. Norouzi & Moghaddam (2020) believe that the entire city of Miandoab sits atop an aquifer fed by nearby mountain ranges, such as Sahand, and major rivers like the Zarrineh Rud. The Miandoab plain, located near the water-abundant Zarrineh Rud and Simineh Rud rivers, generally has a groundwater level fluctuating between 5 and 10 m in depth. The region's lowland geography, along with the Zarrineh Rud flowing through the center of the city, contributes to the high groundwater levels. Based on the groundwater depth at various points and their elevations above sea level, an equipotential map was created using GIS software (Figure 5). The highest elevations are observed in the southern and northeastern points at 1286 and 1288 m. Moving northwest, elevations decrease, indicating proximity of the groundwater to the surface. However, some areas deviate from this pattern; for instance, in the central part of the map, elevations near the river reach 1284 m, while further from the river they drop to 1280 m, indicating groundwater pumping activity.

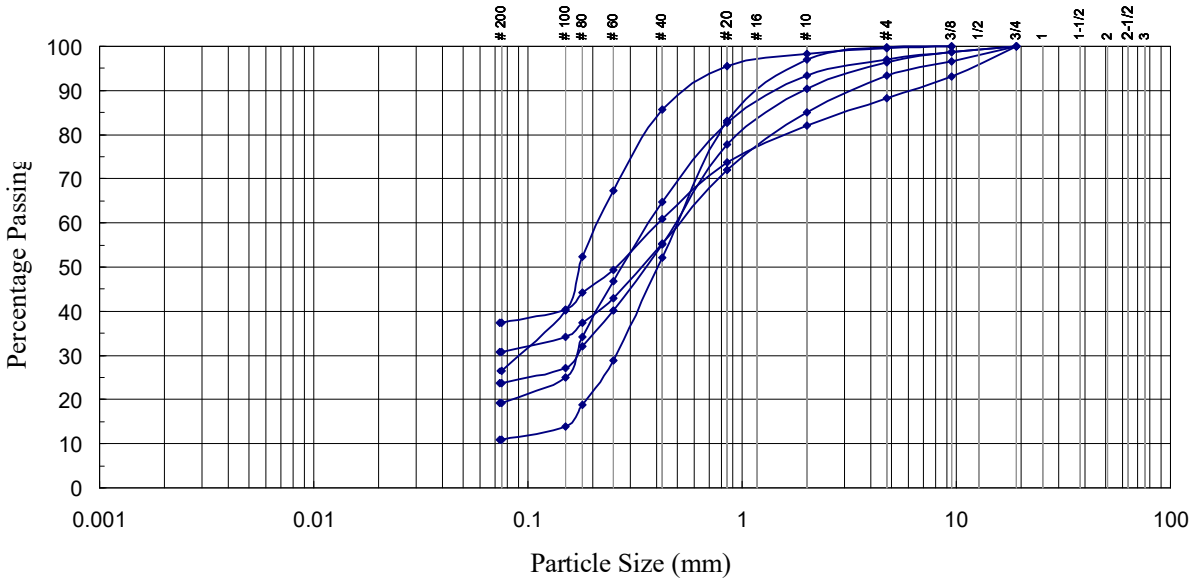

Fig. 3 Particle size diagram of the soils of the region

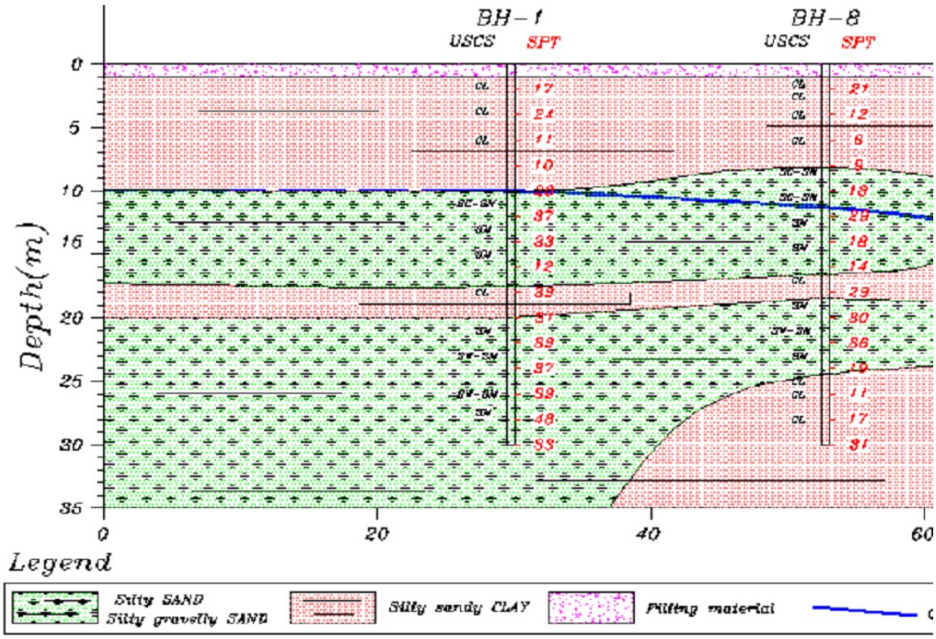

Fig. 4 Geotechnical cross-section of the 350-bed hospital in the east of Miandoab

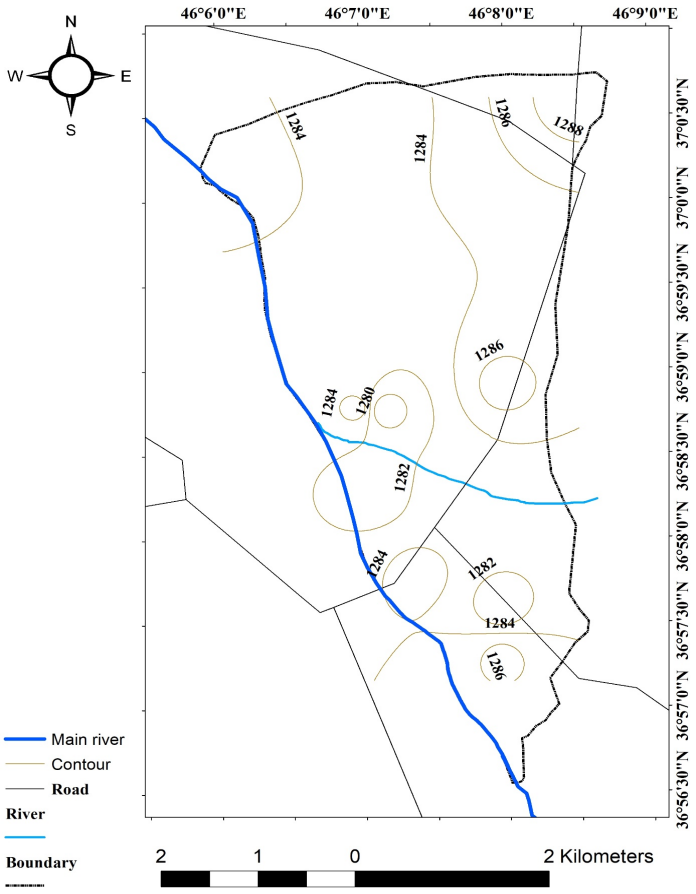

Fig. 5 Alignment map of the underground water level in the east of Miandoab

III. Liquefaction Potential with Empirical Methods

Evaluating soil liquefaction potential is crucial in assessing seismic hazards, especially in earthquake-prone areas (Lin et al., 2004). Empirical methods provide a practical approach to estimate the likelihood of liquefaction by using field data, typically from tests such as the SPT, CPT, and V_s. These methods are often preferred due to their efficiency and the direct insights they offer into soil behavior under seismic loading (Kayen et al., 2013; Zhang & Wang, 2012).

Researchers such as Seed & Idriss (1971) developed a field-based approach for estimating soil liquefaction potential using SPT data, which was later expanded upon by Idriss & Boulanger (2006). In their method, they introduced the concept of cyclic stress ratio (CSR) and utilized soil layer response analysis under seismic vibrations to predict liquefaction potential. The method involves calculating CSR, which represents the earthquake-induced stresses on soil layers, and comparing it to the soil's resistance to liquefaction. This approach has become foundational in liquefaction assessment, with the following formula often used to express their relationship:

$$CSR=\left(\frac{\tau_{ave}}{\sigma'_{v0}}\right)=0.65\left(\frac{a_{\max}}{g}\right).\left(\frac{\sigma_{v0}}{\sigma'_{v0}}\right).r_d \quad (1)$$

where, $a_{\max}$ represents the maximum ground acceleration, g is the acceleration due to gravity, σ_v denotes the total stress, σ'_v is the effective overburden stress of the layer under consideration, and r_d is the stress reduction coefficient. This coefficient accounts for the flexibility of the overburden soil profile and is used to ensure that it behaves appropriately in the calculations. Typically, this coefficient is calculated using depth-related relationships as follows:

$$r_d \rightarrow \begin{cases} 0<z\le 9.15\,m \;\Rightarrow\; r_d=1.0-0.00765z \\ 9.15<z\le 23\,m \;\Rightarrow\; r_d=1.17-0.00267z \end{cases} \quad (2)$$

where, z represents the overburden depth. Idriss & Boulanger (2006) suggest that a soil's resistance to liquefaction can be estimated using the cyclic resistance ratio (CRR), which can be calculated from the corrected SPT value, denoted as N_{60}. The corrected SPT values are obtained based on 60% of the energy from the SPT blows, $(N_{SPT})_{60}$. After making the necessary adjustments, the CRR corresponding to a magnitude 7.5 earthquake ($CRR_{7.5}$) can be derived from the clean sand as $(N_{SPT})_{60cs}$ values. The relationships for calculating the CRR are as follows (Neyromand et al., 2016):

$$CRR_{7.5}=\frac{1}{34-(N_{SPT})_{60cs}}+\frac{(N_{SPT})_{60cs}}{135}+\frac{50}{[10(N_{SPT})_{60cs}+45]^2}-\frac{1}{200} \quad (3)$$

$$CRR=\exp\left(\begin{array}{l}[\frac{(N_{SPT})_{60cs}}{14.1}]+[\frac{(N_{SPT})_{60cs}}{126}]^2- \\ [\frac{(N_{SPT})_{60cs}}{23.6}]^3+[\frac{(N_{SPT})_{60cs}}{25.4}]^4-2.8\end{array}\right) \quad (4)$$

$$(N_{SPT})_{60cs}=(N_{SPT})_{60}+\Delta(N_{SPT})_{60} \quad (5)$$

$$\Delta(N_{SPT})_{60}=1.63+\exp\left(1+\frac{9.7}{FC+0.1}\right)-\left(\frac{15.7}{FC+0.1}\right)^2 \quad (6)$$

where, FC represents the percentage of fine-grained soil at the specified depth, and the ratio of CRR to CSR is referred to as the liquefaction safety factor ($F.S_{liq}$). Liquefaction is likely to occur if $F.S_{liq}$ is less than 1. Another approach is proposed by Youd & Idriss (2001), based on the National Center for Earthquake Engineering Research (NCEER) method, which calculates CSR using the peak horizontal acceleration of the earthquake at the ground surface ($a_{\max}$). Their relationship is expressed as follows (Youd & Idriss, 2001; Cetin et al., 2004):

$$CSR=\left(\frac{\tau_{ave}}{\sigma'_{v0}}\right)=0.65\left(\frac{a_{\max}}{g}\right).\left(\frac{\sigma_{v0}}{\sigma'_{v0}}\right).\frac{r_d}{MSF} \quad (7)$$

In this Eq., MSF represents the magnitude scaling factor, which adjusts for the earthquake magnitude and is calculated using the following formula (Adeli-Gharjedaghi et al., 2011):

$$MSF=\begin{cases}\left[\frac{7.5}{M_w}\right]^{2.95} & \rightarrow M_w\le 7.5 \\ \left[\frac{7.5}{M_w}\right]^{2.65} & \rightarrow M_w>7.5\end{cases} \quad (8)$$

The calculation of CRR based on SPT blows in the NCEER method involves the following steps:

- Identifying the FC and N_{SPT} values for layers that are prone to liquefaction,
- Correcting N_{SPT} based on rod length, sampler type, and borehole diameter. The corrected N_{SPT} for clean sand is then calculated according to FC, following the Seed and Idriss method.

Another approach used in this study is the method by Iwasaki et al. (1984), which builds on Seed & Idriss (1971) method. The Iwasaki et al. (1984) empirical method is one of the widely used approaches. It involves collecting SPT data at various borehole locations, determining the $(N_{SPT})_{60}$ to adjust for energy variations, and then calculating the liquefaction potential index (LPI) for each point. The LPI helps quantify the likelihood and severity of liquefaction across different soil layers, considering factors like soil type, relative density, groundwater level, and expected earthquake magnitude. Iwasaki et al. (1984) method calculates the F.S by dividing the two parameters R by L.

$$R = 0.0882\sqrt{\frac{N}{\frac{\sigma'}{98}+0.7}} + 0.225\log\frac{35}{D_{50}} \quad (9)$$

$$R = 0.0882\sqrt{\frac{N}{\frac{\sigma'}{98}+0.7}} - 0.05 \quad (10)$$

$$L = \frac{a_{\max}a^2 + b^2 = c^2_{\max}}{g}\cdot\frac{\sigma}{\sigma'}\cdot r_d \quad (11)$$

It is worth noting that if D_{50} (the median grain diameter) is between 0.04 and 0.6 mm, Eq. 9 is recommended, and if it falls between 0.6 and 1.5 mm, Eq. 10 is suggested. Finally, the PL value is calculated as.

$$PL = \int_0^{20} F\cdot W(z)dz \quad (12)$$

$$IF \quad F_L < 1 \rightarrow F = 1 - F_L$$
$$IF \quad F_L > 1 \rightarrow F = 0 \quad (13)$$

$$W(z) = 10 - 0.5z \quad (14)$$

In these Eqs., z represents depth. Accordingly, based on the calculated PL value, three conditions apply: if PL is less than 5, the risk of liquefaction is very low for the area; if it is between 5 and 15, the risk is moderate; and if it is greater than 15, the risk of soil liquefaction is considered very high. It should be noted that the empirical methods, while sometimes limited by local soil conditions and uncertainties in estimating seismic forces, remain widely accepted due to their simplicity and field applicability.

IV. Liquefaction Potential of the Region

To assess the liquefaction potential of the study area, field investigations were conducted, and data from 16 boreholes drilled for various projects in eastern Miandoab were collected. The depths of these boreholes range from 10m to 30m, with their locations shown in Figure 6. Among the drilled boreholes, certain soil layers were found to have no liquefaction potential and can be disregarded in this context. However, some boreholes indicate layers with potential liquefaction risk (Pajoohesh Omran Rahvar, 2021).

In the drilled boreholes, variations in the SPT values have been estimated. Table 1 illustrates the changes in SPT values across different boreholes in the study area. Additionally, Table 2 presents the changes in SPT values relative to $(N_{SPT})_{60cs}$. Based on the results from the SPT tests, the liquefaction safety factors for the area under investigation can be calculated using the Iwasaki et al. method. The results of these calculations are provided in Table 3. The variations in the calculated $F.S_{liq}$ for the study area are depicted in Figure 7.

Based on the obtained results and the threshold value for the liquefaction safety factor ($F.S_{liq}$ = 1.0), it can be concluded that the study area exhibits a range from no potential for liquefaction to high potential for liquefaction. Considering the calculated variations through these relationships, a liquefaction hazard map has been developed and is presented in Figure 8. According to the soil types and the results obtained, the central and southern parts of the area face a high risk of liquefaction in the event of an earthquake with a peak ground acceleration exceeding 0.25g and a magnitude greater than 7. Furthermore, using the Iwasaki et al. method, it has been identified that the central sections in eastern Miandoab have a liquefaction risk factor close to 5, indicating a medium risk of liquefaction. Considering the groundwater level and its flow direction from south to north, along with the presence of fine-grained soils up to a depth of approximately 8m, followed by loose, saturated sandy soils, it is essential to conduct drilling for projects in the area down to a depth of 20m. This depth is critical for accurately assessing the geotechnical conditions and potential liquefaction risks associated with construction in the region.

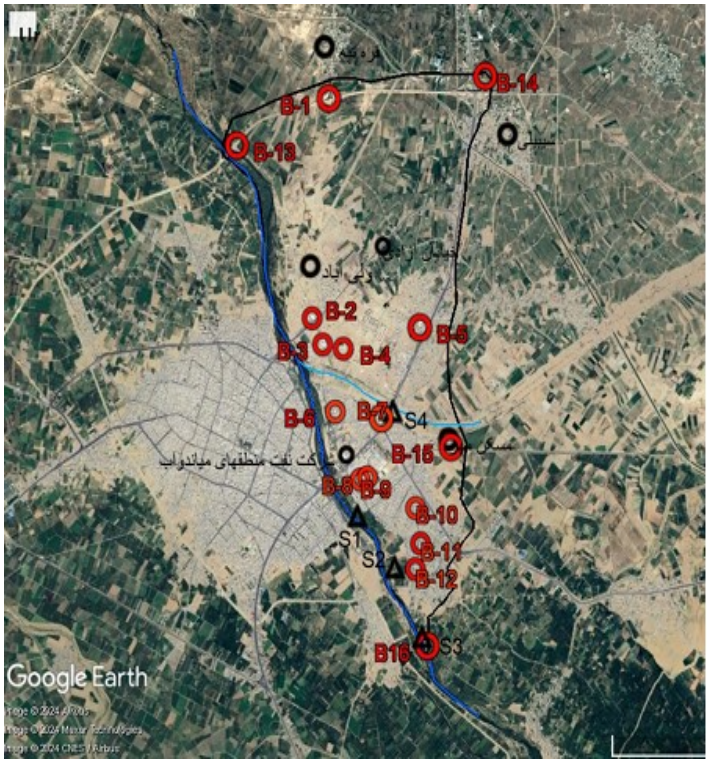

Fig. 6 The position of boreholes in the studied area

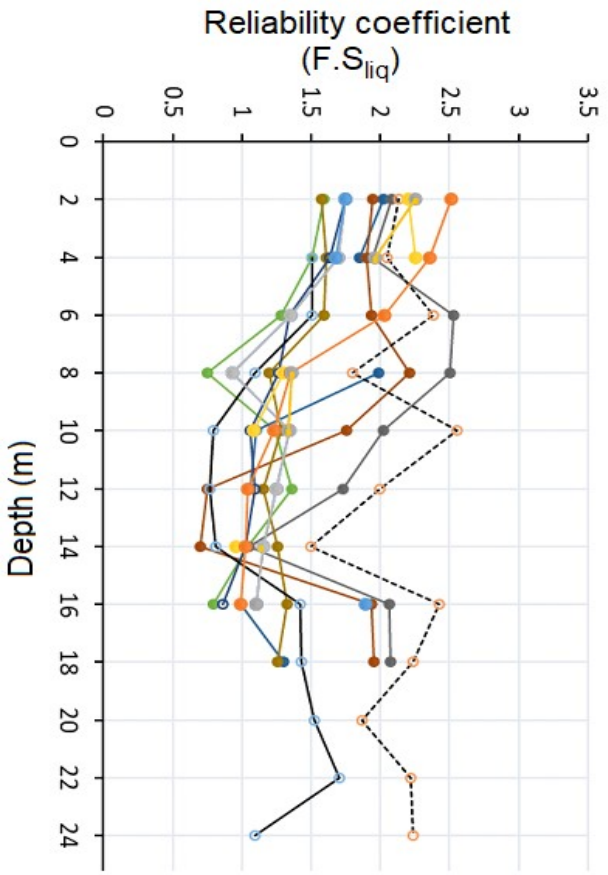

Fig. 7 Variations of soil liquefaction reliability coefficient with respect to depth in different boreholes

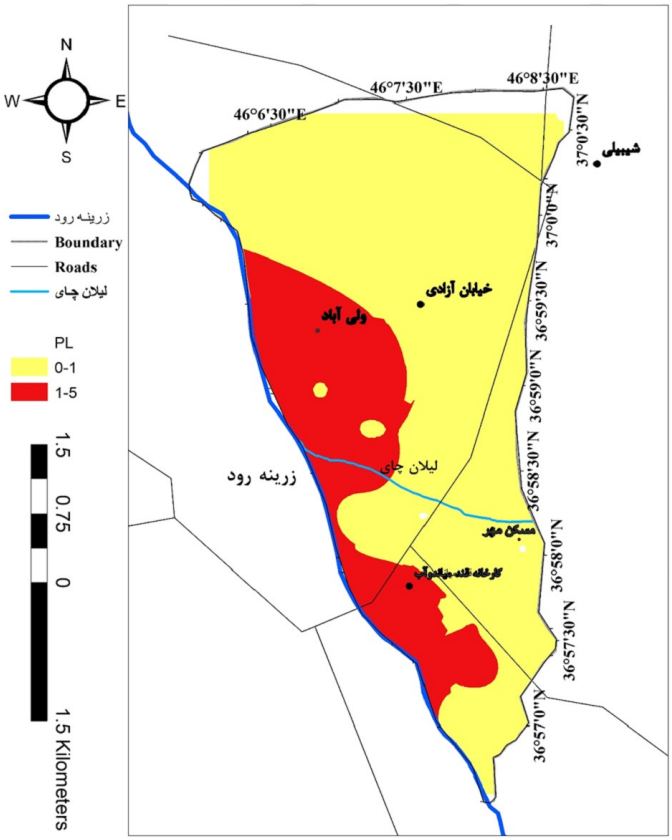

Fig. 8 The liquefaction hazard zoning map for the studied region

Table 1 SPT values variations via depth

Borehole ID	N_{SPT} (m per depth)			
	8	10	12	14
BH01	65	75	18	76
BH02	16	15	18	15
BH03	16	15	17	15
BH04	12	18	18	37
BH05	17	15	16	16
BH06	18	16	17	22
BH07	18	20	17	18
BH08	18	12	11	27
BH09	20	37	33	12
BH10	19	18	16	15
BH11	17	23	16	14
BH12	24	14	18	16
BH13	43	54	16	60
BH14	40	36	17	54
BH15	17	15	18	21
BH16	15	18	17	14

Table 2 Average modified SPT values variations via depth

Depth (m)	N_{SPT}			FL coefficient
	N_{60}	$(N_1)_{60}$	$(N_1$	
2	16.6	36.0	40.3	2.12
4	20.0	30.3	38.5	2.05
6	30.8	38.6	52.9	2.38
8	50.0	53.0	75.7	2.83
10	54.2	59.9	76.5	2.55
12	63.3	71.2	86.1	2.57
14	15.0	22.5	27.3	1.05

Table 3 The $F.S_{liq}$ variations in accordance with Iwasaki method

Depth (m)	L coefficient	R coefficient	FL coefficient
2	0.16	0.34	2.13
4	0.15	0.32	2.05
6	0.15	0.36	2.38
8	0.15	0.43	2.83
10	0.16	0.42	2.55
12	0.16	0.43	2.57
14	0.16	0.17	1.05
16	0.16	0.40	2.43
24	0.12	0.28	2.23
26	0.11	0.21	1.87
28	0.10	0.23	2.22
30	0.09	0.20	2.23

V. CONCLUSION

The study area is located in the Miandoab plain, characterized by alluvial deposits primarily formed by the Zarrineh and Lilan rivers. The topsoil in eastern Miandoab is fine-grained up to a depth of 8 meters, followed by sand and gravel layers, and deeper layers (beyond 35 m) consist of black marl. Groundwater levels range from 5 to 15 meters below the surface, with a general flow direction to the north. Grain size analysis indicates soils with medium plasticity, with a plasticity index between 15 and 25%. According to the Unified Soil Classification System (USCS), the soils are mainly categorized as CL and SM. SPT results show that soils in the central and southern parts are loose to medium, while soils in the northern parts are medium to very dense. Based on Code 2800, the area is in a moderate relative risk zone, with a design base acceleration of 0.25g. An

earthquake with 0.25g acceleration and magnitude 7 could induce liquefaction to a depth of 15 meters, with lower liquefaction risk expected in northern areas. Fine-grained soils in this area show minimal liquefaction potential. Due to an 8-meter-thick non-liquefiable fine-grained layer at the surface, sand liquefaction at depths of 8 to 15 meters would likely not significantly impact shallow foundations up to a ground acceleration of 0.30g. In seismic conditions, the primary geotechnical hazard includes liquefaction, which this study aimed to assess using SPT values based on the Iwasaki method. Results indicate low to very low liquefaction potential across most points, although some depths show a factor of safety below one. Detailed liquefaction hazard assessments are recommended for major projects in the region.

ACKNOWLEDGMENT

We extend our thanks to the reviewers for their meticulous attention to detail and constructive suggestions that greatly improved the quality of this manuscript. Your contributions have been instrumental in shaping this work.

AUTHORS' CONTRIBUTIONS

Armin Moazafarbaygi conducted the main data analysis, contributed to the data collection, preprocessing, and interpretation, and was responsible for drafting the initial manuscript. Ebrahim Asghari-Kaljahi assisted in the development of the methodology and performed validation checks, provided supervision, conceptual guidance, and critical revision of the manuscript. All authors read and approved the final manuscript.

CONFLICT OF INTEREST

The authors have not disclosed any competing interests.

OPEN ACCESS

REFERENCES

Adeli-Gharjedaghi F., Dabiri R., Bonab, M.H. (2011). Comparison of Liquefaction Potential Assessment Using Cone Penetration Test (CPT) and Shear Wave Velocity (Vs) Methods Based on Empirical Relationships in Southern Tehran. *Journal of Hydraulic Structures Engineering*, 3(5), 36-46.

Andabili N.R., Safaripour M. (2022). Identification of precipitation trend and landslide susceptibility analysis in Miandoab County using MATLAB. *Environmental Monitoring and Assessment*, 194(7), 472. https://doi.org/10.1007/s10661-022-10069-w.

Asgari S. (2017). A General Review of Soil Liquefaction and Mitigation Methods. In: *Proceedings of the 5th International Congress on Civil Engineering, Architecture, and Urban Development*, Tehran, Iran.

Azarafza M., Mokhtari M.H. (2013). Evaluation of drought effect on Urmia Lake salinity changes using remote sensing techniques. *Journal of Arid Biome*, 3(2), 1-14.

Baez J.I., Martin G.R., Youd T.L. (2000). Comparison of SPT-CPT liquefaction evaluations and CPT interpretations. *Innovations and Applications in Geotechnical Site Characterization*, pp. 17-32. https://doi.org/10.1061/40505(285)2.

Boulanger R.W., Idriss I.M. (2014). *CPT and SPT based liquefaction triggering procedures*. Report No. UCD/CGM.-14, 1, 134.

Cetin K.O., Seed R.B., Der Kiureghian A., Tokimatsu K., Harder Jr L.F., Kayen R.E., Moss R.E. (2004). Standard penetration test-based probabilistic and deterministic assessment of seismic soil liquefaction potential. *Journal of Geotechnical and Geoenvironmental Engineering*, 130(12), 1314-134. https://doi.org/10.1061/(ASCE)1090-0241(2004)130:12(1314).

Cetin K.O., Seed R.B., Kayen R.E., Moss R.E., Bilge H.T., Ilgac M., Chowdhury K. (2018). Examination of differences between three SPT-based seismic soil liquefaction triggering relationships. *Soil Dynamics and Earthquake Engineering*, 113, 75-86. https://doi.org/10.1016/j.soildyn.2018.03.013.

Demir S., Özener P. (2022). Effect of shear strain compatibility and incompatibility approaches in the design of high modulus columns against liquefaction: A case study in Christchurch, New Zealand. Bulletin *of Earthquake Engineering*, 20, 5721-5745. https://doi.org/10.1007/s10518-022-01427-7.

Farhangi V., Karakouzian M., Geertsema M. (2020). Effect of micropiles on clean sand liquefaction risk based on CPT and SPT. *Applied Sciences*, 10(9), 3111. https://doi.org/10.3390/app10093111.

Fazlnia A. (2019). Geochemical and tectonic significance of the Arbat alkali gabbro-monzonite-syenite intrusions, Urumieh-Dokhtar Magmatic Arc, Iran. *Geological Quarterly*, 63(1), 16-29. http://dx.doi.org/10.7306/gq.1449.

Geological Survey and Mineral Exploration of Iran, GSI (2009). *Geology map and report for Miandoab region*. The Geological Survey and Mineral Exploration of Iran press, Tehran, Iran.

Huang Y., Bao Y., Zhang M., Liu C., Lu P. (2015). Analysis of the mechanism of seabed liquefaction induced by waves and related seabed protection. *Natural Hazards*, 79, 1399-1408. https://doi.org/10.1007/s11069-015-1897-1.

Huang Y., Yu M. (2013). Review of soil liquefaction characteristics during major earthquakes of the twenty-first century. *Natural Hazards*, 65, 2375-2384. https://doi.org/10.1007/s11069-012-0433-9.

Idriss I.M., Boulanger R.W. (2006). Semi-empirical procedures for evaluating liquefaction potential during earthquakes. *Soil Dynamics and Earthquake Engineering*, 26(2-4), 115-130. https://doi.org/10.1016/j.soildyn.2004.11.023.

Iranian Code of Practice for Seismic Resistance Design of Buildings (2014). *Standard No. 2800 (4th Edition)*. Building and Housing Research Center. Theran, Iran.

Iwasaki T., Arakawa T., Tokida K. (1984), Simplified procedures for assessing soil liquefaction during earthquakes, *International Journal of Soil Dynamics and Earthquake Engineering*, 3(1), 49-58, https://doi.org/10.1016/0261-7277(84)90027-5.

Kayen R., Moss R.E.S., Thompson E.M., Seed R.B., Cetin K.O., Kiureghian A. D., Tokimatsu K. (2013). Shear-wave velocity–based probabilistic and deterministic assessment of seismic soil liquefaction potential. *Journal of Geotechnical and Geoenvironmental Engineering*, 139(3), 407-419. https://doi.org/10.1061/(ASCE)GT.1943-5606.0000743.

Lenz J.A., Baise L.G. (2007). Spatial variability of liquefaction potential in regional mapping using CPT and SPT data. *Soil Dynamics and Earthquake Engineering*, 27(7), 690-702. https://doi.org/10.1016/j.soildyn.2006.11.005.

Lin C.P., Chang C.C., Chang T.S. (2004). The use of MASW method in the assessment of soil liquefaction potential. Soil *Dynamics and Earthquake Engineering*, 24(9-10), 689-698. https://doi.org/10.1016/j.soildyn.2004.06.012.

Neyromand A., Dabiri R., Razizadeh F.B. (2016). Comparison of Liquefaction Potential Assessment in Soil Layers of Southwestern Ahar Region Based on Standard Penetration Resistance and Shear Wave Velocity Methods. *Journal of Seismology and Earthquake Engineering*, 19(1), 23-37.

Norouzi H., Moghaddam A.A. (2020). Groundwater quality assessment using random forest method based on groundwater quality indices (case study: Miandoab plain aquifer, NW of Iran), *Arabian Journal of Geosciences*, 13, 912. https://doi.org/10.1007/s12517-020-05904-8.

Norouzi H., Moghaddam A.A. (2022). Determining the origin of arsenic anomalies in groundwater using multivariate statistical methods (case study: Miandoab plain aquifer, NW of Iran). *Environmental Earth Sciences*, 81(10), 301. https://doi.org/10.1007/s12665-022-10385-x.

Ortiz-Hernández E., Chunga K., Pastor J.L., Toulkeridis T. (2022). Assessing Susceptibility to Soil Liquefaction Using the Standard Penetration Test (SPT)- A Case Study from the City of Portoviejo, Coastal Ecuador. *Land*, 11(4), 463. https://doi.org/10.3390/land11040463.

Pajoohesh Omran Rahvar (2021). *Geotechnical and Foundation Engineering Consulting Report for the 350-Bed Miandoab Hospital Project*. Organization for the Execution of State Buildings, Ministry of Housing and Urban Development, 63 p.

Seed H.B., Idriss I.M. (1971). Simplified procedure for evaluating soil liquefaction potential. *Journal of the Soil Mechanics and Foundations Division*, 97(9), 1249-1273. https://doi.org/10.1061/JSFEAQ.0001662.

Vaziri M., Mahmoudi S., Shahbazi F., Masihabadi M.H., Rezaei H. (2022). Towards a Sustainable Agriculture Development Based on the Field Vulnerability Evaluation in Miandoab Region, Iran. *Nexo Revista Científica*, 35(04), 950-960. https://doi.org/10.5377/nexo.v35i04.15533.

Xu C., Feng C., Du X., Zhang X. (2020). Study on liquefaction mechanism of saturated sand considering stress redistribution. *Engineering Geology*, 264, 105302. https://doi.org/10.1016/j.enggeo.2019.105302.

Xu Y.H., Li M.F. (2021). Hydrothermal liquefaction of lignocellulose for value-added products: Mechanism, parameter and production application. *Bioresource Technology*, 342, 126035. https://doi.org/10.1016/j.biortech.2021.126035.

Youd T.L. (2003). Liquefaction mechanisms and induced ground failure. *International Geophysics*, 81, 1159-1173. https://doi.org/10.1016/S0074-6142(03)80184-5.

Youd T.L., Idriss I.M. (2001). Liquefaction Resistance of Soils: Summary Report from the 1996 NCEER and 1998 NCEER/NSF Workshops on evaluation of Liquefaction resistance of soils. *Journal of Geotechnical and Geoenvironmental Engineering*, 127(4), 297-313. https://doi.org/10.1061/(ASCE)1090-0241(2001)127:10(817).

Zhang J.M., Wang G. (2012). Large post-liquefaction deformation of sand, part I: physical mechanism, constitutive description and numerical algorithm. *Acta Geotechnica*, 7, 69-113. https://doi.org/10.1007/s11440-011-0150-7.

Zhao X., Cai G. (2015). SPT-CPT correlation and its application for liquefaction evaluation in China. *Marine Georesources & Geotechnology*, 33(3), 272-281. https://doi.org/10.1080/1064119X.2013.872740.